Academic Journal of Science and Technology
ISSN: 2771-3032 | Vol. 11, No. 3, 2024

Fabricating Fine-Grained Copper Foil by Ultrafine Anode Scanning Electrodeposition without Using Additives

Lunxu Li *

School of Mechanical and Power Engineering, Henan Polytechnic University, Jiaozuo Henan, 454000, China
*** Corresponding author:** Lunxu Li

Abstract: Copper foil, recognized for its excellent electrical conductivity, malleability, and corrosion resistance, is widely used in various applications, notably in lithium-ion batteries and printed circuit boards. However, decomposition products from organic additives often decrease its electrical performance. This study introduces ultrafine anode scanning electrodeposition (UAS-ECD), a new method that firms copper foils without organic additives. Increased scanning speed enhances the diffusion of copper ions and reduces concentration polarization but also loosens the deposition layer, decreasing the tensile strength and surface quality of the copper foil. Increased current density leads to decreased surface quality, finer grain size, and increased tensile strength. Experimental results indicate that utilizing the concentrated current density and the significant local overpotential characteristics of line anode ultrafine anode scanning electroplating can prepare high-purity copper foil, approximating the performance of high-performance electroplated copper without additives.

Keywords: Electrodeposition; Ultrafine Anode Scanning Electrodeposition; Fine-Grained; Additives; Copper Foils.

1. Introduction

Copper foil, a fundamental material in the modern electronics industry, has seen increasing demand thanks to the flourishing development of the sector [1-6]. Lithium-ion copper foil is mainly used in lithium-ion batteries as the current collector. Thinner and lighter copper foil reduces the weight of lithium-ion batteries, increasing their energy density[7]; Higher tensile strength and improved corrosion resistance enhance the cycling performance of lithium-ion batteries. Lower roughness reduces the internal resistance of lithium-ion batteries, enhances coulombic efficiency, and improves the safety of lithium-ion batteries by reducing the risk of puncture[8,9]. As the demand for lighter, thinner, denser, and safer lithium-ion batteries increases in the electric vehicle industry, there is greater emphasis on the requirements for lithium-ion copper foil thickness, tensile strength, and surface roughness. This demand has increased the need for high-end copper foil products[10,11].

The predominant method for preparing lithium-ion copper foil is currently the rod-to-roller electroplating process, noted for its simple manufacturing process and high production efficiency. Adding trace additives to the electrolyte is the most effective method for controlling the performance of electrolytic copper foil[12-15]. In the electrodeposition process, additives do not simply add up; they interact synergistically, compete, and collectively influence the outcome[16-18]. However, introducing additives inevitably introduces impurity elements into the electrodeposited metal layer[19]. Moreover, in the electrodeposition process for preparing lithium-ion copper foil, the extremely high current density (≥ 40 A/dm²) causes organic additives to decompose. The decomposition products are difficult to remove, and their residues can lead to defects like wrinkling, band breakage, orange peel, blistering, and pinholes in the copper foil[20-22].Furthermore, balancing multiple additives is necessary to enhance the performance of copper foil while avoiding adverse effects[23]. This partially increases the maintenance cost of the electrolyte system for the electrodeposition process used in lithium-ion copper foil[24].

Therefore, to ensure the purity and performance of copper foil while avoiding the negative impact of additives, a new electrodeposition method is needed[25,26]. The Ultrafine Anode Scanning Electrodeposition (UAS-ECD) technique is a novel method proposed by the author's team in recent years, distinguished by its unique operational approach. This technique focuses the current on the ultrafine anode surface to achieve ultra-high overpotential, promoting crystal nuclei formation and resulting in finer crystallization[27]. Therefore, ultrafine anode scanning electrodeposition technology can replace the grain refinement effect of additives in traditional electrolytic copper foil preparation methods. This enables the production of ultra-fine grain copper foil without additives. Additionally, process efficiency can be improved by arranging the ultrafine anodes in an array. This study offers a new approach for preparing high-performance copper strips.

2. Experimental

2.1. Materials and Methods

Fig 1 shows the theoretical model of the ultrafine anode scanning electrodeposition technology. A thin inert anode is embedded into a rigid stirring paddle exposing only a fine ultrafine area (thickness or diameter, $d \leq 50$ μm). After polishing to a smooth finish, the anode and the stirring paddle form an ultrafine anode-stirring paddle assembly. This assembly is then placed close to the cathode surface for linear reciprocating scanning movements.

Unlike traditional surface area electrodeposition methods, the ultrafine anode scanning electrodeposition technology uses a small anode area, so the applied voltage/current is highly concentrated on the ultrafine anode surface. Additionally, due to the small working gap, the voltage/current radiates to the cathode surface. The radiated

region's area is related to the size of the working gap. In ultrafine anode scanning electrodeposition, the metal forming mechanism significantly differs from traditional electrodeposition methods. On one hand, ultrafine anode scanning electrodeposition exhibits highly concentrated voltage/current. The continuous anode movement results in different mass transfer effects. Therefore, under such circumstances, the electrolyte composition and core process parameters need to be re-matched to ensure ultra-high current density during processing for grain refinement. Additionally, the goal is to reduce grain growth time, achieving ultra-fain grain copper foil preparation. Therefore, this paper focuses on studying the effects of core process parameters on the surface quality, microstructure, and mechanical properties of copper foil, and optimizing the process conditions.

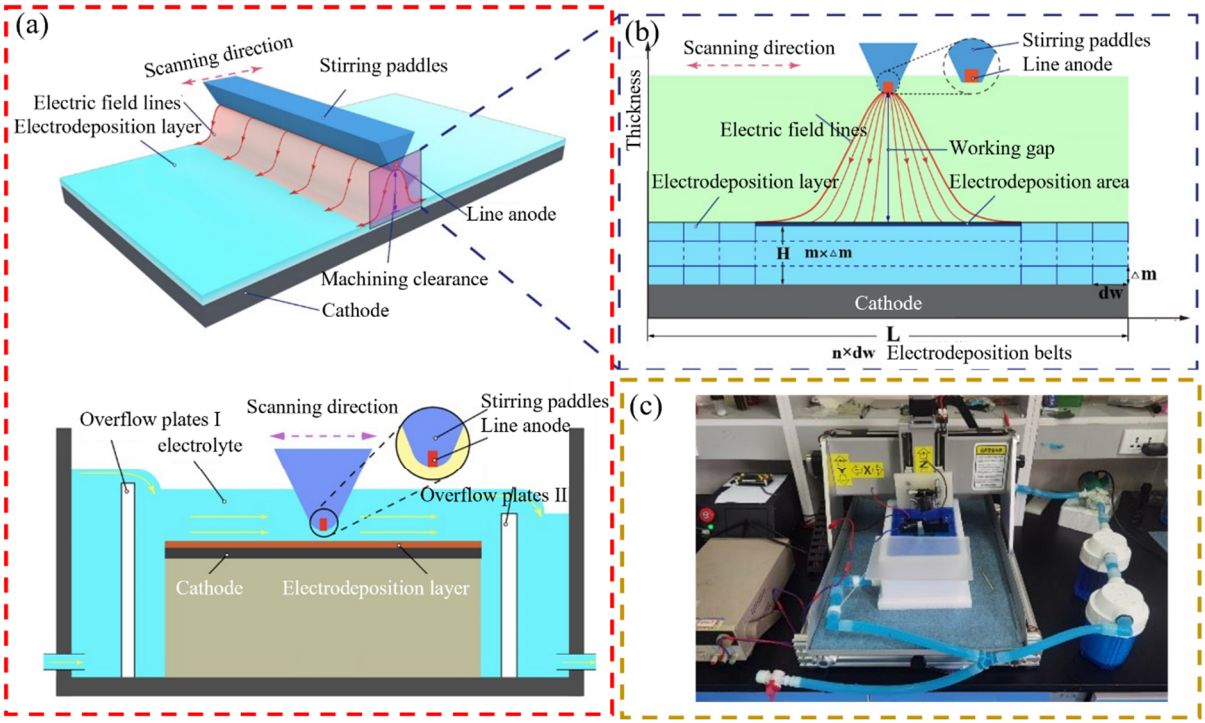

Figure 1. Schematic diagram of UAS-ECD:(a) Schematic drawings of UAS-ECD, (b)Mechanism diagram of UAS-ECD, (c)Picture of UAS-ECD device

Figure 1 shows the ultrafine anode scanning electrodeposition system used in the experiment The experimental system includes a three-dimensional motion platform, solution tank, filter, magnetic pump, moving slide table, stirring paddle, ultrafine anode, precision power supply, and computer. During the electrodeposition process, the electrolyte circulates through a magnetic pump, passes through a filter, and then re-enters the solution tank, ensuring electrolyte circulation and renewal. The solution level in the tank is controlled by an overflow mode, and the flow rate is adjusted by regulating valves. This mode ensures prompt renewal of the solution at the processing site. The solution level in the tank is controlled by an overflow mode, and the flow rate of the solution is adjusted by regulating valves. This mode ensures prompt renewal of the solution at the processing site. The three-dimensional motion platform enables the reciprocating movement of the anode, adjusting its position relative to the cathode to maintain the working gap. Additionally, a slide table device ensures that the ultrafine anode and cathode surfaces are parallel and enables finer and more precise control of the working gap.

The anode material is a platinum sheet with 99.99% purity, measuring 100 mm in length, 10 mm in width, and 50 μm in thickness. It is embedded in acrylic, exposing an ultrafine anode of 100 mm in length and 50 μm in thickness, which is polished to a smooth finish. High-purity titanium is used as the cathode, with a conductive area of 40 mm × 40 mm. The conductive area of the anode is 40 mm in length, with a scanning stroke of 40 mm. The working gap is 500 μm.

Before electrodeposition, the cathode with the exposed square deposition area was fixed face-up in the solution tank. The anode was positioned so that its lower surface was parallel to the upper surface of the cathode. The anode-stirrer assembly was then adjusted to maintain a 500-micron processing gap between the lower surface of the anode and the upper surface of the cathode. The scanning stroke of the moving platform was adjusted so that the anode's motion path matched the width of the cathode's deposition area, with the anode's linear motion endpoint aligned with the two edges of the square deposition area. The rectangular path formed by the anode's scanning motion was parallel to and directly above the cathode area.

The electrolyte is a sulfate electrodeposition solution system, with good solution stability. Additionally, its simple composition facilitates analysis and control, with fewer operational constraints. Since the anode is an inert and insoluble, it cannot replenish the consumed copper ions during the electrodeposition process. Therefore, the solution must be sufficiently abundant to minimize the impact of metal ion depletion on the electrodeposition process. Additionally, by monitoring the coulombs consumed, copper sulfate is promptly added to maintain the main salt concentration and avoid experimental interference. The specific electrolyte composition is copper sulfate (CuSO4) 290 g/L (provided by Tianjin Kermio Chemical Reagent Co., Ltd.) and sulfuric acid (H2SO4) 60 g/L (provided by Tianjin Kermio Chemical Reagent Co., Ltd.). Electrolyte circulation is performed for 10-15 minutes before electrodeposition. During the

electrodeposition process, the temperature is maintained at 25±0.5°C. The thickness is controlled by electrodeposition time calculated using Faraday's law of electrolysis.

During the single-factor experiment on scanning speed, the inter-electrode current was kept constant at 0.32 A. During the single-factor experiment on inter-electrode current, the scanning speed was kept constant at 10 mm/s.

Table 1. Electrolyte composition

Ingredient	Content
CuSO4 · 5H2O (g/L)	290
H2SO4 (g/L)	60

Table 2. Experimental parameters

Process parameters	The numerical
Inter-electrode currents (i, A)	0.1,0.2,0.3,0.4,0.5
Scanning speeds (V, mm/s)	1,5,10,15,20
working gap (D, um)	500
temperature (°C)	25±0.5°

2.2. Analysis and Testing Methods

The macroscopic morphology of the copper foil was observed using an automated image measuring instrument (AM600). The microscopic morphology was examined with a scanning electron microscope (Merlin Compact). Surface roughness was measured using a laser confocal microscope (OLS5100). Before observation, the surface was cleaned with a 5% sulfuric acid solution to remove the oxide layer, then rinsed with deionized water and air-dried at room temperature. Crystal orientation analysis was performed using a rotating anode X-ray diffractometer (Smart Lab) with Cu Kα radiation, wavelength λ=0.152 nm, grazing incidence angle of 2°, scanning speed of 10°/min, and a scanning range of 35° to 85°. The texture coefficient (TC) characterized the preferred orientation of crystal planes in different samples.

$$TC = \frac{I_{(hkl)}/I_0(hkl)}{\sum_{i=1}^{n} I_{(hkl)}/I_{0(hkl)}} \times 100\%$$

In the formula: $I(hkl)$ represents the diffraction intensity of the crystal plane of the sample, $I_0(hkl)$ represents the diffraction intensity of the crystal plane of the standard sample, and n is the total number of crystal planes studied. The Scherrer formula was used to calculate the grain size.

$$D = \frac{K\gamma}{B\cos\theta}$$

In the formula, K is the Scherrer constant, γ is the X-ray wavelength, B is the full width at half maximum of the diffraction peak of the sample, and θ is the Bragg diffraction angle.

Dumbbell-shaped tensile specimens were prepared using a manual hydraulic punch machine (YL-15 type). The tensile strength of the copper foil was tested using an electronic universal testing machine (WDW-05+). The tensile test was conducted according to the standard GB/T228.1-2010 "Metallic Materials - Tensile Testing at Ambient Temperature" with a tensile speed of 0.5 mm/s. The tensile strength (σ) was calculated using the following formula:

$$\sigma = \frac{F_b}{S_0}$$

Where Fb is the peak force at the fracture of the specimen, and $S0$ is the original cross-sectional area of the specimen.

3. Results and Discussion.

3.1. Surface Quality

Surface morphology observations and roughness measurements of the deposited layer at different scanning speeds in Figure 2 (a-f) show that at a scanning speed of 1 mm/s, the surface roughness is 0.575 μm. However, numerous micro-columns, nodules, and pits present on the surface of the deposited layer. At a scanning speed of 2 mm/s, although there are no obvious pits on the copper foil surface, the surface texture is relatively loose, with a surface roughness of 0.682 μm. As the scanning speed increases to 10 mm/s, the crystals on the copper foil surface become smaller, but the bonding of the deposited layer becomes looser, resulting in a surface roughness of 0.745 μm. Furthermore, at a scanning speed of 20 mm/s, the unevenness of the copper foil surface increases, with uneven crystal distribution, resulting in a surface roughness of 1.256 μm.

The scanning speed significantly impacts the surface morphology of the copper foil. At low scanning speeds resulting in a longer residence time of the anode in the electroplating area. Consequently, the same area receives current for a longer duration. However, the agitation effect at low speeds is poor, meaning the copper ion concentration in the cathode area cannot meet long-term electroplating requirements, resulting in significant concentration polarization and vigorous hydrogen evolution. Additionally, due to the smaller working gap and slower stirring speed, electrolyte agitation on the electrolytic surface is weak, causing bubbles to accumulate on the electrode surface, These bubbles are difficult to remove and tend to adsorb on the cathode surface, hindering copper deposition. Furthermore, bubbles generated by the anodic oxygen evolution reaction accumulate between the two electrodes, causing more pits on the copper foil surface and a rough deposition layer. As the scanning speed increases, the anode's residence time in the electroplating area decreases, and the stirrer's agitation of the electrolyte on the cathode surface strengthens, leading to better mass transfer and reduced concentration polarization. Additionally, the stirrer's agitation of the electrolyte reduces bubble accumulation on the electrode surface, minimizing their impact on the electroplating process and resulting in a denser copper deposition layer. As the scanning speed further increases, although the mass transfer effect improves, the anode's residence time in the electroplating area decreases further, causing some areas of the cathode surface to have insufficient time for copper ion deposition. Microscopically, this uneven crystal distribution is observed on the electroplated copper layer's surface.

Figures 2 (g-l) illustrate the surface morphology and roughness of the deposited layer at different current densities. The figures show that as the current density increases, the quality of the deposited layer gradually deteriorates. The surface roughness of the deposited layer increases from 0.472 μm at 0.1 A to 2.145 μm at 0.5 A, with a gradual increase in circular pits. During the electrodeposition process, the cathode surface undergoes not only the reduction of metal ions to metal atoms (the main reaction), but also the reduction of hydrogen ions to evolve hydrogen gas (the side reaction). The increase in current density accelerates the consumption of metal atoms on the cathode surface, resulting in insufficient local supply of metal ions and exacerbating concentration polarization. This intensifies the hydrogen evolution side reaction of the electrodeposition process. Excessive hydrogen

evolution can lead to voids in the deposited layer formed by hydrogen gas bubbles, or the temporary adhesion of hydrogen gas on the cathode surface without timely expulsion. At this point, hydrogen gas bubbles hinder the subsequent electrodeposition process, forming circular pits on the deposited layer's surface. Additionally, the surface morphology of the deposited layer is influenced by local current density. The small processing gap results in a significant increase in local current density with increasing current from the power source. As a result, grain growth accelerates in a specific direction, ultimately leading to the formation of a rough surface on the deposited layer.

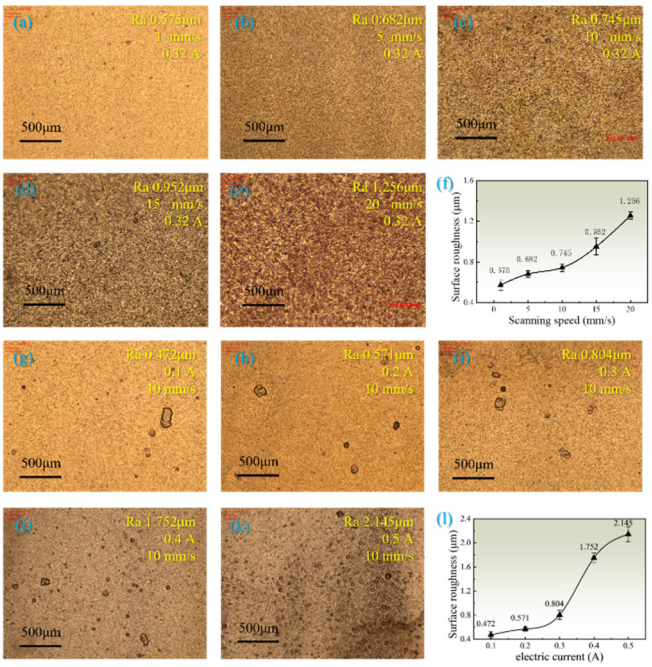

Figure 2. Macroscopic morphology and surface roughness of deposition layers

Yan Xiao et al. studied the effects of 3,3'-Dithiobis-1-propanesulfonic acid disodium salt (SPS), gelatin, and sodium thiazoline dithiopropane sulfonate (SH110) on the morphology, roughness, and peel strength of HVLP copper foil [28]. The results showed that gelatin was the most effective in reducing the surface roughness of copper foil, but the optimal surface roughness was still 1.58 μm, significantly higher than the 0.472 μm achieved in this study. This indicates that this method can significantly improve the surface quality of copper foil without the use of additives.

Figure 3 (a-e) shows the surface microstructure of the copper foil deposited at different scanning speeds. The surface microstructure of the deposited layer does not change significantly at different scanning speeds.

However, in terms of grain size, at the same inter-electrode current, the scanning speed affects the copper foil's processing effect by influencing the metal electrocrystallization process during deposition. During electrodeposition, metal ions move through the electrolyte to the cathode surface and reduce to metal atoms. Newly adsorbed metal atoms exhibit two behaviors as they diffuse along the electrode surface: (1) they diffuse into the existing metal lattice, and (2) they aggregate with other newly formed atoms to create and grow nuclei. These concurrent behaviors ultimately form crystals. The rates of these concurrent behaviors determine the grain size of the electroplated layer. If the nucleation rate of metal atoms is fast and the nuclei growth rate is slow during electrodeposition, many small grains will form. Conversely, if the nucleation rate is slow and the nuclei growth rate is fast, larger grains will form. The faster the scanning speed, the smaller the grain size of the nickel deposition layer. This is because higher current density at faster scanning speeds promotes the formation of new nuclei, while the increased speed hinders the growth of these nuclei. Therefore, faster scanning speeds result in smaller grain sizes.

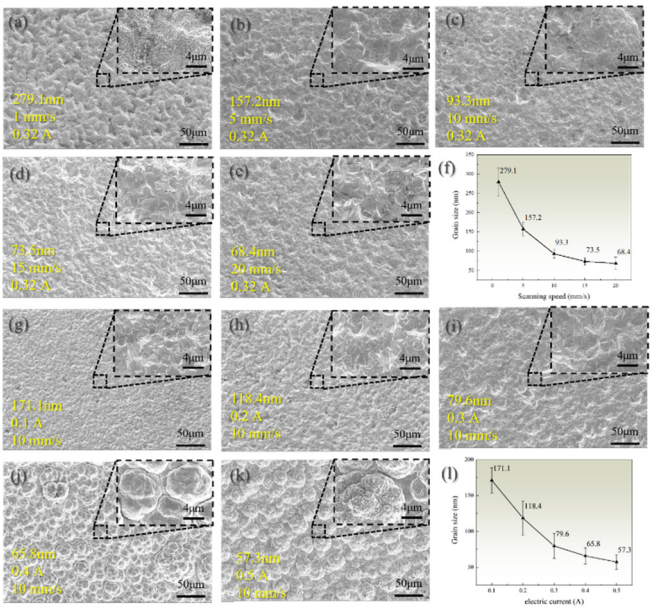

Figure 3. SEM images and grain size of deposition layers at different output currents and scanning speeds

Figures 3 (g-k) show the microsurface morphology of copper foil under different inter-electrode currents. When the inter-electrode current is 0.1 A, a pyramid-like structure forms on the copper foil surface, and appears relatively sharp. As the inter-electrode current increases from 0.1 A to 0.2 A, the pyramid-like structures on the surface decrease in number and size but still exist. Further increasing the inter-electrode current to 0.3 A gradually diminishes these structures, with the sharp peaks becoming smoother, and the surface structure tending towards a spherical shape. When the inter-electrode current further increases to 0.5 A, the pyramid-like structures on the copper foil surface completely disappear, transitioning into numerous cluster structures. At relatively low inter-electrode currents, the mass transfer effect at this current density is sufficient to support the electrodeposition process. Additionally, due to the low inter-electrode current, the overpotential on the cathode surface is small, providing less driving force for the electrode process. Consequently, the electrocrystallization process of the metal mostly occurs through screw dislocation growth, leading to the formation of pyramid-like shapes on the copper foil surface. As the inter-electrode current increases, the cathodic overpotential increases, providing greater driving force for the electrode process. The metal electrocrystallization process then occurs mainly through nucleation. Additionally, due to the higher current density on the cathode surface, metal crystallization occurs rapidly, resulting in insufficient copper ions on the cathode surface, which enhances concentration polarization. The hydrogen evolution reaction intensifies, forming numerous spherical particles on the cathode surface. Over time, these small particles connect, forming cluster structures.

Additionlly, the adsorption of tiny hydrogen bubbles on the cathode surface results in the presence of voids between clusters and on the surface.

Figure 3(l) shows that as the current increases, the grain size of the copper foil continuously decreases. With the gradual increase in output current, the grain size of the deposited layer gradually decreases. The grain size of the deposited layer decreases from 171.1 nm at 0.1 A to 57.3 nm at 0.5 A. This is because as the current increases, the current density also increases, raising the cathodic overpotential and resulting in smaller grain sizes. Figure 3(f) shows that as the scanning speed increases, the grain size decreases. When the scanning speed increases from 1 mm/s to 10 mm/s, the grain size decreases from 279.1 nm to 93.3 nm. As the ultrafine anode continuously moves, a slower speed means it stays longer on a unit length of the area, ensuring sufficient energy supply. This allows crystals to sustain growth, resulting in larger grain sizes. Conversely, a faster scanning speed shortens the stay time on a unit area, leading to shorter crystal growth time and smaller grain sizes [29]. During the electrodeposition process, faster scanning speeds result in smaller grain sizes of the deposited layer. This is because at higher scanning speeds, the excessively high current density of the ultrafine anode promotes the formation of new crystal nuclei, and the increased speed hinders their growth. Consequently, faster scanning speeds lead to smaller grain sizes. This principle aligns with the fundamentals of ultrafine anode scanning electroplating.

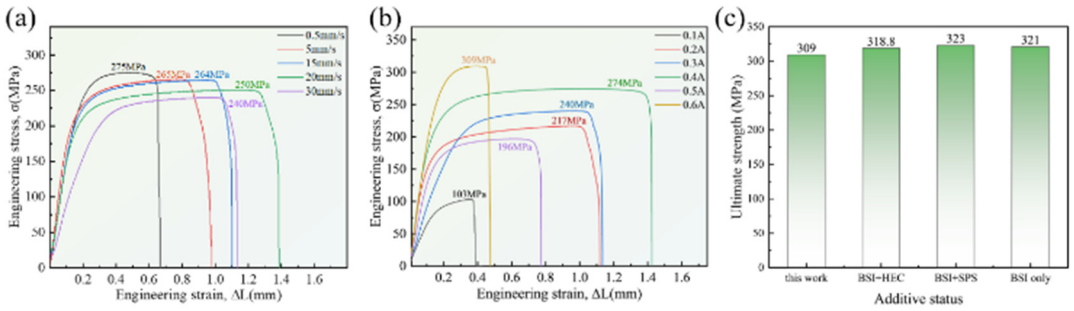

Figure 4. Tensile strength of deposition layers at different output currents and scanning speeds and comparison with conventional methods [31]

3.2. Mechanical Properties

Figure 4(a) shows that at an inter-electrode current of 0.1 A, the tensile strength of the copper foil is lowest at 103 MPa, with poor ductility. As the inter-electrode current increases, the tensile strength of the copper foil increases, and its ductility improves. At 0.4 A, the tensile strength reaches 274 MPa, and its ductility is optimal. However, as the inter-electrode current increases to 0.5 A, the tensile strength begins to decrease, and ductility worsens. When the inter-electrode current rise to 0.6 A, the tensile strength increases again, but ductility further deteriorates.

When the inter-electrode current is low and the anode in the wire scanning electrodeposition constantly moves, the current at the electrodeposition position is small and transient, resulting in low overpotential on the cathode surface. The nuclei formed during the electrocrystallization process cannot exist stably and dissolve back into the solution, resulting in a slow deposition rate. Additionally, influenced by the characteristics of wire scanning electrodeposition, the deposited layer consists of multiple micro-metal layers/bands connected. The current density is low, results in a slow deposition rate and poor connection accuracy between each micro-metal layer/band, leading to a relatively loose texture . Consequently, the tensile strength and ductility are low. As the inter-electrode current increases, sufficient energy is invested in the electrodeposition process. The nuclei can exist stably, and there is enough energy to support grain growth. Hence, the deposition rate increases, the connection accuracy improves, and the copper foil becomes denser. Consequently, the tensile strength and ductility increase. When the inter-electrode current further increases, the cathode surface current density rises. At this point, mass transfer cannot provide sufficient copper ion deposition, leading to severe hydrogen evolution. Clustering structures appear on the copper foil surface, making the texture porous. Consequently, the tensile strength decreases again, and the ductility worsens. As the inter-electrode current continues to increase, exceeding the threshold within this gap, more charring appears on the copper foil surface. The increased charring causes the copper foil to become brittle. Therefore, this explains why the tensile strength of the copper foil initially increases, then decreases, and then increases again with the rise in inter-electrode current [30].

Figure 4(b) shows that when the scanning speed is 0.5 mm/s, the tensile strength of the copper foil is maximum at 275 MPa, but the elongation at break is relatively low. As the scanning speed increases, the tensile strength of the copper foil gradually decreases, while the elongation at break increases. When the scanning speed is 20 mm/s, the tensile strength is 250 MPa, representing the best balance of properties. However, with a further increase in scanning speed, the tensile strength slightly decreases to 240 MPa, accompanied by a decrease in elongation at break.

The tensile strength of the deposited layer at different scanning speeds is generally high (≥240 MPa) due to the high inter-electrode current used during the single-factor experiment for scanning speed. The high current increased the cathodic overpotential, refining the grains and resulting in higher tensile strength of the copper foil. On one hand, the increased scanning speed causes some nuclei to dissolve back into the solution due to insufficient energy supply, changing the deposition method from dense layered stacking to loose bulk accumulation. This looseness leads to decreased tensile strength. On the other hand, the increased scanning speed hinders grain growth, positively affecting grain refinement. Smaller grain size increases the tensile strength of the deposited layer. Combining these effects, the final tensile strength of the deposited layer shows a decreasing trend with increasing scanning speed.

Figure 4(c) compares the tensile strength of the copper foil deposited in this study under optimized parameters with

results from other studies. Y. Sun, J. Pan, and L. Liu prepared copper foil using conventional deposition methods with organic additives BSI, SPS, and HEC, achieving a tensile strength slightly higher than that in this study. However, the use of organic additives in their process reduced the copper foil's purity [31].

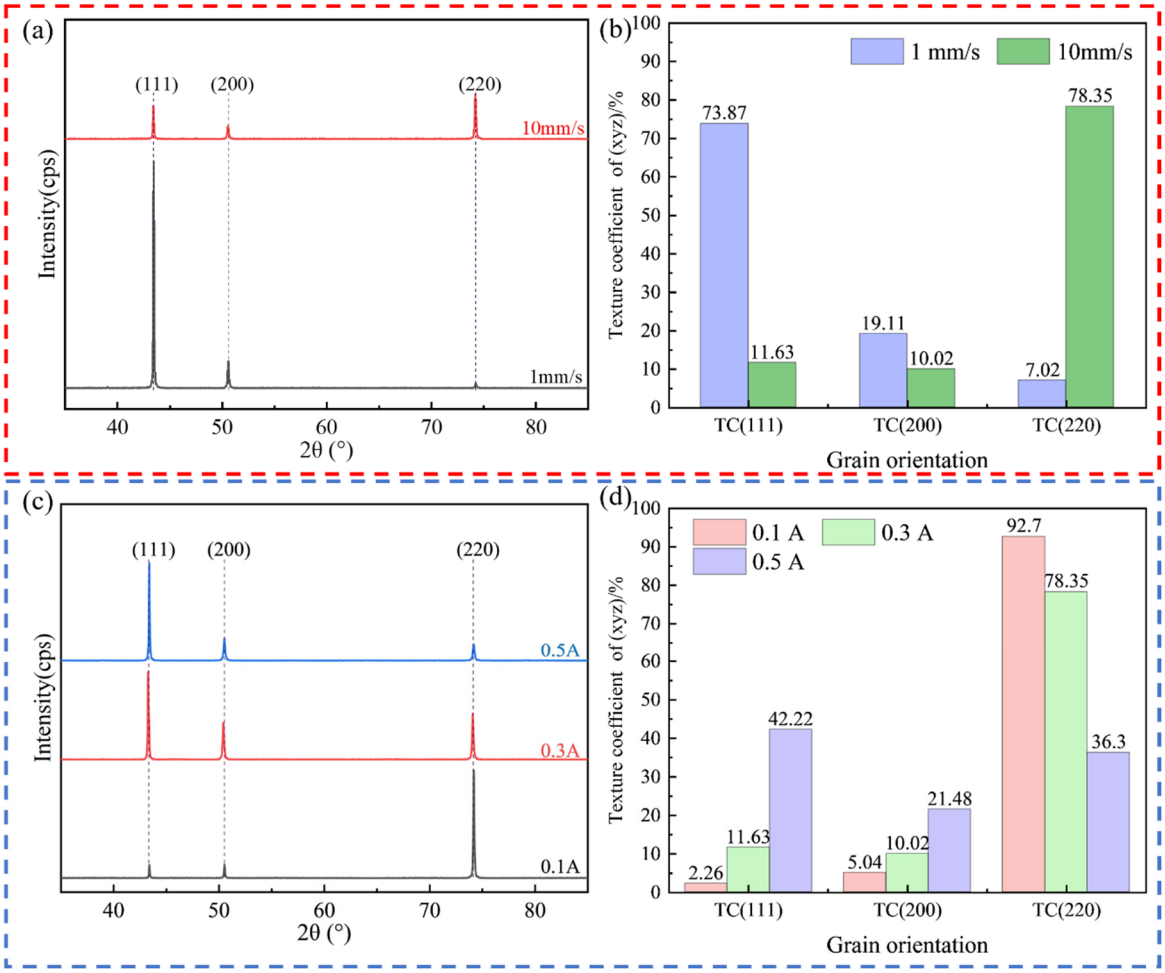

Figure 5. Crystallographic orientation of deposition layers at different output currents and scanning speeds

3.3. Microstructural Organization

Figure 5 (a, b) shows the grain orientation of the deposited layer at different scanning speeds. At a scanning speed of 1 mm/s, the preferred orientation is the (111) plane, with TC(111) being 73.87%. When the scanning speed increases to 10 mm/s, the preferred orientation of the copper foil changes from the (111) crystal plane to the (220) crystal plane. TC(220) is 78.35%, and the orientations of the (111) and (200) crystal planes are approximately equal, with TC(111) and TC(200) being 11.63% and 10.02%, respectively.

Figure 5 (c, d) shows the grain orientation of the deposited layer at different current densities. At an inter-electrode current of 0.1 A, the copper foil exhibits a preferred orientation with the (220) plane. The texture coefficient TC(220) is 92.7%, while the orientations of the (111) and (200) planes are not prominent, with TC(111) and TC(200) being 2.26% and 5.04%, respectively. With the inter-electrode current increasing to 0.3 A, the copper foil still exhibits a preferred orientation with the (220) crystal plane, the proportion has relatively decreased, with TC(220) being 78.35%. The orientations of the (111) and (200) planes are approximately equal, with TC(111) and TC(200) being 11.63% and 10.02%, respectively. With the inter-electrode current further increasing to 0.5 A, the preferred orientation of the copper foil shifts from the (220) crystal plane to the (111) crystal plane. However, the difference between the two orientations is not significant, with TC(111) and TC(200) being 42.22% and 36.30% respectively.

According to electrodeposition nucleation theory, the nucleation rate is inversely proportional to the energy required for nucleation. Copper has a face-centered cubic structure, and the nucleation energy of the (220) crystal plane is lower than that of the (111) plane. When the scanning speed is slow, the anode stays in the same area as the cathode for a longer time, allowing the cathode to receive energy for a longer duration. The (111) crystal plane has good symmetry and relatively stable structure, consuming energy during the electrocrystallization process by forming (111) planes. As the scanning speed increases, the anode spends less time in the same area as the cathode, resulting in less energy being received there. Therefore, the deposition mainly occurs on the (220) plane. Further increasing the anode speed enhances the prominence of the (220) crystal plane orientation[31].

4. Conclusion

This study presents a novel ultrafine anode scanning electrodeposition method to prepare high-performance fine-grained copper foil without additives. The main processing parameters were experimentally investigated for their effects on the grain size, tensile strength, and surface roughness of the deposited layer, along with an analysis of their operating principles. The results indicate that as the scanning speed increases, the tensile strength of the deposited layer decreases,

with increasing current, the tensile strength of the deposited layer increases. At an output current of 0.6A and a scanning speed of 10 mm/s, copper foil with a tensile strength of 309 MPa was prepared. As the scanning speed and current increase, the surface roughness of the deposited layer increases. The surface roughness of the copper foil prepared under the conditions of a current of 0.1 A and a scanning speed of 10 mm/s is 0.472 μm. Experimental results demonstrate that this method can achieve surface roughness and tensile strength levels comparable to conventional electrodeposition methods with additive assistance, under conditions of no additive assistance. Further analysis reveals that as the scanning speed and current increase, the grain size of the deposited layer gradually decreases. At a current of 0.5 A and a scanning speed of 10 mm/s, copper foil with an average grain size of 57.3 nm was prepared. This explains the improvement in mechanical properties of the deposited layer. Therefore, utilizing this technique enables the preparation of high-performance fine-grained copper foil without additives. This study provides a novel approach for preparing high-performance copper strips.

Credit Authorship Contribution Statement

Lunxu Li: Writing – original draft, Writing – review & editing.

Declaration of Competing Interest

The authors declare that they have no known competing financial interests or personal relationships that could have appeared to influence the work reported in this paper.

Acknowledgments

This work was supported by the National Natural Science Foundation of China (Grant number 51875178).

References

[1] J. Reid, Copper electrodeposition: principles and recent progress, Japanese Journal of Applied Physics, 40(4S) (2001) 2650. https://doi.org/10.1143/JJAP.40.2650

[2] W. Li, L. Liu, C. Zhong, B. Shen, W. Hu, Effect of carbon fiber surface treatment on Cu electrodeposition: The electrochemical behavior and the morphology of Cu deposits, Journal of Alloys and Compounds, 509(8) (2011) 3532-3536. https://doi. org/ 10.1016/j.jallcom.2010.12.170

[3] M.W. Lane, C.E. Murray, F.R. McFeely, P.M. Vereecken, R. Rosenberg, Liner materials for direct electrodeposition of Cu, Applied Physics Letters, 83(12) (2003) 2330-2332. https:// doi.org/10.1063/1.1610256

[4] J.J. Jhan, K. Wataya, H. Nishikawa, C.M. Chen, Electrodeposition of nanocrystalline Cu for Cu-Cu direct bonding, Journal of the Taiwan Institute of Chemical Engineers, 132 (2022) 104127. https://doi.org/10.1016/j.jtice.2021.10.027

[5] T. Gao, G. Meng, J. Zhang, et al., Template synthesis of single-crystal Cu nanowire arrays by electrodeposition, Applied Physics A, 73 (2001) 251-254. https://doi.org/ 10.1007/ s003390100910

[6] P.C. Andricacos, Copper on-chip interconnections: A breakthrough in electrodeposition to make better chips, The Electrochemical Society Interface, 8(1) (1999). https://doi. org/ 32. 10.1149/2.F06991IF

[7] K. Jagannadham, Thermal Conductivity of Copper-Graphene Composite Films Synthesized by Electrochemical Deposition with Exfoliated Graphene Platelets, Metallurgical and Materials Transactions B, 43 (2012) 316-324. https://doi.org/ 10.1007/s11663-011-9597-z

[8] K. Tamakawa, K. Sakutani, H. Miura, Effect of micro texture of electroplated copper thin films on their mechanical properties, Zairyo/Journal of the Society of Materials Science, Japan, 56(10) (2007) 907-912. https://doi.org/ 10.2472/ jsms.56.907

[9] W. Peng, J. Gao, T. Lu, B. Sun, X. Zhang, L. Zhang, S. Tu, Insights into abnormal grain growth in copper thin films for reduced electrical resistivity: A quantitative multi-order-parameter phase-field study under finite element framework, Acta Materialia, 260 (2023) 119236. https://doi.org/ 10. 1016/j.actamat.2023.119236

[10] M.J. Kim, S.K. Cho, H.C. Koo, T. Lim, K.J. Park, J.J. Kim, Pulse electrodeposition for improving electrical properties of Cu thin film, Journal of the Electrochemical Society, 157(11) (2010) D564. https://doi.org/10.1149/1.3481564

[11] H.S. Kim, S.R. Dhage, D.E. Shim, Intense pulsed light sintering of copper nanoink for printed electronics, Applied Physics A, 97 (2009) 791-798. https://doi.org/10.1007/s00339-009-5360-6

[12] M.J. Kim, S. Choe, H.C. Kim, S.K. Cho, S.-K. Kim, J.J. Kim, Electrochemical behavior of citric acid and its influence on Cu electrodeposition for damascene metallization, Journal of the Electrochemical Society, 162(8) (2015) D354. https://doi. org/10.1149/2.0561508jes

[13] M.J. Kim, H.C. Kim, J.J. Kim, The influences of iodide ion on Cu electrodeposition and TSV filling, Journal of the Electrochemical Society, 163(8) (2016) D434. https://doi.org/ 10.1149/ 2.1111608jes

[14] J.J. Kelly, C. Tian, A.C. West, Leveling and microstructural effects of additives for copper electrodeposition, Journal of the Electrochemical Society, 146(7) (1999) 2540. https://doi. org/ 10. 1149/1.1391968

[15] Y.J. Han, X. Zhang, G.W. Leach, Shape control of electrodeposited copper films and nanostructures through additive effects, Langmuir, 30(12) (2014) 3589-3598. https:// doi. org/ 10.1021/la500001j

[16] M. Hasan, J.F. Rohan, Cu electrodeposition from methanesulfonate electrolytes for ULSI and MEMS applications, Journal of the Electrochemical Society, 157(5) (2010) D278. https://doi.org/10.1149/1.3332729

[17] O. Ghodbane, L. Roue, D. Belanger, Copper electrodeposition on pyrolytic graphite electrodes: Effect of the copper salt on the electrodeposition process, Electrochimica Acta, 52(19) (2007) 5843-5855. https://doi.org/10.1016/j.electacta.2007.03.009

[18] M.A. Pasquale, L.M. Gassa, A.J. Arvia, Copper electrodeposition from an acidic plating bath containing accelerating and inhibiting organic additives, Electrochimica Acta, 53(20) (2008) 5891-5904. https:// doi.org/ 10.1016/ j.electacta.2008.03.073

[19] Y.E. Jo, D.Y. Yu, S.K. Cho, Revealing the inhibition effect of quaternary ammonium cations on Cu electrodeposition, Journal of Applied Electrochemistry, 50 (2020) 245-253. https://doi. org/ 10.1007/s10800-019-01381-4

[20] P.T. Lee, Y.S. Wu, P.C. Lin, C.C. Chen, W.Z. Hsieh, C.E. Ho, High-speed Cu electrodeposition and its solderability, Surface and Coatings Technology, 320 (2017) 559-567. https://doi.org/ 10.1016/j.surfcoat.2016.11.016

[21] S.K. Kim, J.J. Kim, Superfilling evolution in Cu electrodeposition: dependence on the aging time of the

accelerator, Electrochemical and Solid-State Letters, 7(9) (2004) C98. https://doi.org/10.1149/1.1777552

[22] T.T. Hoang, S. Ma, J.I. Gold, P.J. Kenis, A.A. Gewirth, Nanoporous copper films by additive-controlled electrodeposition: CO2 reduction catalysis, ACS Catalysis, 7(5) (2017) 3313-3321. https://doi.org/10.1021/acscatal.6b03613

[23] L. Bonou, M. Eyraud, R. Denoyel, Y. Massiani, Influence of additives on Cu electrodeposition mechanisms in acid solution: direct current study supported by non-electrochemical measurements, Electrochimica Acta, 47(26) (2002) 4139-4150. https://doi.org/10.1016/S0013-4686(02)00356-0

[24] P. Sebastián, E. Vallés, E. Gómez, Copper electrodeposition in a deep eutectic solvent: First stages analysis considering Cu (I) stabilization in chloride media, Electrochimica Acta, 123 (2014) 285-295. https://doi.org/10.1016/j.electacta.2014.01.062

[25] W.Y. Ko, W.H. Chen, C.Y. Cheng, et al., Architectural Growth of Cu Nanoparticles Through Electrodeposition, Nanoscale Research Letters, 4 (2009) 1481. https://doi.org/ 10.1007/ s11671-009-9424-5

[26] M.R. Majidi, K. Asadpour-Zeynali, B. Hafezi, Reaction and nucleation mechanisms of copper electrodeposition on disposable pencil graphite electrode, Electrochimica Acta, 54(3) (2009) 1119-1130. https://doi.org/ 10.1016/j. electacta. 2008. 08. 035

[27] N.D. Nikolić, K.I. Popov, L.J. Pavlović, M.G. Pavlović, Morphologies of copper deposits obtained by the electrodeposition at high overpotentials, Surface and Coatings Technology, 201(3-4) (2006) 560-566. https://doi. org/10. 1016/j.surfcoat.2005.12.004

[28] Y. Xiao, W.C. Sun, Z.B. Bai, et al., Effect of additives on microstructure and properties of the coarsened layer of very low profile (HVLP) copper foil, J. Appl. Electrochem. 53 (2023) 2331–2346. https://doi.org/10.1007/s10800-023-01930-y

[29] D. Grujicic, B. Pesic, Electrodeposition of copper: the nucleation mechanisms, Electrochimica Acta, 47(18) (2002) 2901-2912. https://doi.org/10.1016/S0013-4686(02)00161-5

[30] M. Hakamada, Y. Nakamoto, H. Matsumoto, H. Iwasaki, Y. Chen, H. Kusuda, M. Mabuchi, Relationship between hardness and grain size in electrodeposited copper films, Materials Science and Engineering: A, 457(1-2) (2007) 120-126. https://doi.org/10.1016/j.msea.2006.12.101

[31] Y. Sun, J. Pan, L. Liu, et al., Improvement of performance stability of electrolytic copper foils by bi-component additives, Journal of Applied Electrochemistry, 52 (2022) 1219-1230. https://doi.org/10.1007/s10800-022-01707-9

[32] S. Hwang, I. Oh, J. Kwak, Electrodeposition of Epitaxial Cu(111) Thin Films on Au(111) Using Defect-Mediated Growth, Journal of the American Chemical Society, 123(29) (2001) 7176-7177. https://doi.org/10.1021/ja015666n.